06

Changing the parameters of vacancy formation and self-diffusion in various polymorphic modifications of iron

© M.N. Magomedov

Institute for Geothermal Problems and Renewable Energy — branch of the Joint Institute for High Temperatures of RAS,
367030 Makhachkala, Russia
e-mail: mahmag4@mail.ru

Received July 25, 2022
Revised November 29, 2022
Accepted November 29, 2022

The activation parameters for various iron structures were calculated by the analytical method based on the paired four-parameter Mie−Lennard-Jones interatomic interaction potential. Within the framework of a single method, all the activation processes parameters were calculated: Gibbs energy, enthalpy, entropy and volume for both the process of electroneutral vacancy formation and for the process of atom self-diffusion. The isobaric temperature dependences of the indicated activation parameters for BCC and FCC iron structures from $T = 10$ to 1810 K along two isobars: $P = 0$ and 10 GPa were calculated. It is shown that at the $\alpha-\gamma$ transition temperature (1184 K), the activation parameters decrease during the isobaric transition from the BCC to the FCC structure. At the $\gamma-\delta$ transition temperature (1667 K), the activation parameters increase during the transition from the FCC to the BCC structure. With increasing pressure, the jumps magnitude for the Gibbs energy and the enthalpy of the activation process increases, and for the entropy and volume of the activation process decreases. It is shown that, at low temperatures, due to quantum regularities, activation parameters strongly depend on temperature, and the entropy of activation processes in this region is negative. In the high temperature region, a good agreement has been obtained with the experimental estimates of activation parameters for different iron structures known from the literature.

Keywords: vacancy, self-diffusion, interatomic potential, iron, structure, phase transition.

DOI: 10.21883/TP.2023.02.55474.190-22

Introduction

In terms of the metals distribution in the earth's crust, iron (Fe) occupies the second place after aluminum, so iron is studied for a long time, but some of its properties were studied relatively little. Difficulties in the study are due to the fact that iron at different temperatures (T) and pressures (P) can have a different crystal structure. It is known that at low pressures ($P = 1$ atm) solid iron can exist in three crystalline modifications [1,2]:

1. At low temperatures: $T \le T_{\alpha-\gamma} = 1184 \pm 1$ K, the α-Fe phase with a body-centered cubic (BCC) structure is stable: $k_n = 8$, $k_p = 0.6802$, where k_n — the first coordination number, k_p — packing index of the structure. In α-phase at the Curie temperature $T_C = 1043$ K, a second kind phase transition from the ferromagnetic to the paramagnetic state occurs in iron.

2. In the temperature range: $T_{\alpha-\gamma} \le T \le T_{\gamma-\delta} = 1667 \pm 1$ K, γ-Fe phase with a face-centered cubic (FCC) structure is stable: $k_n = 12$, $k_p = 0.7405$.

3. At high temperatures: $T_{\gamma-\delta} \le T \le T_m = 1811 \pm 3$ K, δ-Fe phase with BCC structure is stable. Here T_m is melting temperature.

Activation parameters (i.e., the parameters of formation of electrically neutral vacancies and self-diffusion of atoms) in various polymorphic modifications of iron were studied for a long time, but to date, reliable experimental data were obtained only for enthalpy (h_i) and volume (v_i) of activation process [3–11]. Yet, there are no methods for measuring or calculating the entropy (s_i) and associated Gibbs energy ($g_i = h_i - Ts_i$) of the activation process [7–11]. Here the index is $i = v$ or d for the formation of electrically neutral vacancies or for the self-diffusion of atoms, respectively. Computer simulation methods allowed us to estimate the values of h_i and v_i at $T = 0$ K, while these data are very contradictory [3–5,7,9]. In papers [8,10] methods were proposed for taking into account the temperature dependence of activation parameters, but these methods are approximate, since they do not take into account the equations of state, thermal expansion, and crystal compressibility.

In this regard, in this paper, the thermal and barometric dependences of all activation parameters in various polymorphic modifications of iron are calculated by the analytical method. The isobaric temperature dependences of the functions g_i, h_i, s_i, and v_i, starting from $T = 10$ K and up to the iron melting point, are calculated for the first time under a standard method. In this case, all calculations were performed along two isobars: at „zero" pressure ($P \approx 10^{-4}$ GPa ≈ 1 atm), where experimental estimates of activation parameters were obtained, and at $P = 10$ GPa.

1. Method of activation parameters calculation

Let us represent a single crystal of a single-component substance from N atoms as a structure of $N+N_v$ cells having the same size, where N_v cells are vacant and uniformly distributed across crystal volume V. We will assume that atoms in the system can be in two states: localized and delocalized. In localized state the atom is in a cell formed by the nearest neighbors and has only the oscillatory degrees of freedom. In delocalized state the atom has access to the whole system volume and has only the translational degrees of freedom.

We will assume that an atom can leave a cell if the amplitude of its oscillation in a cell exceeds $c_o/2$, where $c_o = [6k_pV/(\pi N)]^{1/3}$ — distance between the centers of the nearest cells in an initial (not relaxed into the state activated by vacancies) vacancy-free (at $N_v = 0$) virtual lattice (this is indicated by the index „o“). Here k_p – is the packing index of the structure of $N+N_v$ spherical cells. Then, for the probability of vacancy formation, the following expression was obtained [12]:

$$\phi_v = \frac{N_v}{N+N_v} = 1 - \mathrm{erf}\left[\left(\frac{E_v}{k_\mathrm{B}T}\right)^{1/2}\right], \tag{1}$$

where k_B — Boltzmann's constant, the probability integral has the form

$$\mathrm{erf}(x) = \frac{2}{\pi^{1/2}}\int\limits_0^x \exp(-t^2)dt. \tag{2}$$

In formula (1), the function E_v is the energy of a vacant cell creation in vacancy-free lattice, which has the form [12]:

$$E_v = \frac{m}{k_n^\mathrm{o}}\left(\frac{3c_\mathrm{o}k_\mathrm{B}\Theta_\mathrm{o}}{8\hbar}\right)^2 f_y\left(\frac{3\Theta_\mathrm{o}}{4T}\right). \tag{3}$$

Here $\hbar$ — Planck's constant, m — atomic mass, k_n^o — number of all cells (both occupied and vacant) closest to a given atom, Θ_o — the Debye temperature in vacancy-free lattice (hence the index „o“). The function $f_y(y_w)$ appears in (3) due to quantum effects and has the form

$$f_y(y_w) = \frac{2}{y_w}\frac{[1-\exp(-y_w)]}{[1+\exp(-y_w)]},\ y_w = \frac{3\Theta_\mathrm{o}}{4T}. \tag{4}$$

The probability of atom delocalization is defined as the relative fraction of excited atoms that have a kinetic energy above the threshold E_d — energy of atom delocalization in the bulk of the crystal:

$$x_d = \frac{N_d}{N} = \frac{2}{\pi^{1/2}}\int\limits_{E_d/(k_\mathrm{B}T)}^{\infty} t^{1/2}\exp(-t)dt$$

$$= 2\left(\frac{E_d}{\pi k_\mathrm{B}T}\right)^{1/2}\exp\left(-\frac{E_d}{k_\mathrm{B}T}\right) + 1 - \mathrm{erf}\left[\left(\frac{E_d}{k_\mathrm{B}T}\right)^{1/2}\right]. \tag{5}$$

The delocalization energy of atom is related to the energy of vacant cell by creation by the following relationship:

$$E_d = \left(\frac{3}{8\pi^2}\right)m\left(\frac{3c_\mathrm{o}k_\mathrm{B}\Theta_\mathrm{o}}{4\hbar k_p^{1/3}}\right)^2 f_y(y_w) = C_{ld}E_v, \tag{6}$$

where the structural parameter is introduced:

$$C_{ld} = \frac{3k_n^\mathrm{o}}{2\pi^2 k_p^{2/3}} > 1.$$

In [12] expressions were obtained for the Gibbs energy (g_i), enthalpy (h_i), entropy (s_i) and volume (v_i) similarly to the process of formation of electrically neutral vacancies ($i = v$), and for the process of atom self-diffusion ($i = d$) over the bulk of crystal. Under the condition $E_v \gg k_\mathrm{B}T$ (which is valid for metals up to the melting point), these formulas have the following form:

for the vacancy formation process

$$g_v = -k_\mathrm{B}T\ln(\phi_v) = E_v\left[1 + \left(\frac{k_\mathrm{B}T}{2E_v}\right)\ln\left(\frac{\pi E_v}{k_\mathrm{B}T}\right)\right],$$

$$h_v = E_v\left\{1 - t_y(y_w) + \alpha_p T\left[\left(2 - t_y(y_w)\right)\gamma_\mathrm{o} - \frac{2}{3}\right]\right\},$$

$$\frac{s_v}{k_\mathrm{B}} = \frac{h_v - g_v}{k_\mathrm{B}T} = \frac{E_v}{k_\mathrm{B}T}\left\{\alpha_p T\left[\left(2 - t_y(y_w)\right)\gamma_\mathrm{o} - \frac{2}{3}\right] - t_y(y_w) - \left(\frac{k_\mathrm{B}T}{2E_v}\right)\ln\left(\frac{\pi E_v}{k_\mathrm{B}T}\right)\right\},$$

$$\frac{v_v}{v_0} = \frac{E_v}{B_T v_0}\left[\left(2 - t_y(y_w)\right)\gamma_\mathrm{o} - \frac{2}{3}\right]; \tag{7}$$

for the self-diffusion process

$$g_d = -k_\mathrm{B}T\ln(x_d) = E_d\left[1 - \left(\frac{k_\mathrm{B}T}{2E_d}\right)\ln\left(\frac{4E_d}{\pi k_\mathrm{B}T}\right)\right],$$

$$h_d = E_d\left\{1 - t_y(y_w) + \alpha_p T\left[\left(2 - t_y(y_w)\right)\gamma_\mathrm{o} - \frac{2}{3}\right]\right\},$$

$$\frac{s_d}{k_\mathrm{B}} = \frac{h_d - g_d}{k_\mathrm{B}T} = \frac{E_d}{k_\mathrm{B}T}\left\{\alpha_p T\left[\alpha_p T\left(2 - t_y(y_w)\right)\gamma_\mathrm{o} - \frac{2}{3}\right] - t_y(y_w) + \left(\frac{k_\mathrm{B}T}{2E_d}\right)\ln\left(\frac{4E_d}{\pi k_\mathrm{B}T}\right)\right\},$$

$$\frac{v_d}{v_0} = \frac{E_d}{B_T v_0}\left[\left(2 - t_y(y_w)\right)\gamma_\mathrm{o} - \frac{2}{3}\right]. \tag{8}$$

Here $\alpha_p = (1/V)(\partial V/\partial T)_P$ — isobaric coefficient of thermal expansion, $B_T = -V(\partial P/\partial V)_T$ — isothermal modulus of elasticity, $\gamma_\mathrm{o} = -[\partial\ln(\Theta_\mathrm{o})/\partial\ln(V)]_T$ — first Grüneisen parameter for a vacancy-free crystal, v_0 — volume per atom at $P = 0$ and $T = 0\,\mathrm{K}$,

$$t_y(y_w) = -\frac{\partial\ln(f_y)}{\partial\ln(y_w)} = 1 - \frac{2y_w\exp(y_w)}{[\exp(2y_w) - 1]}. \tag{9}$$

Let us represent the pair interatomic interaction as four parametric Mie–Lennard-Jones potential, which has the form

$$\varphi(r) = \frac{D}{(b-a)}\left[a\left(\frac{r_\mathrm{o}}{r}\right)^b - b\left(\frac{r_\mathrm{o}}{r}\right)^a\right], \qquad (10)$$

where D and r_o — depth and coordinate of the potential minimum, $b > a > 1$ — parameters.

Then, as shown in [13], Debye temperature within the framework of approximation of „only nearest neighbors interaction" can be determined as follows

$$\Theta_\mathrm{o}(k_n^\mathrm{o}, c_\mathrm{o}) = A_w(k_n^\mathrm{o}, c_\mathrm{o})\xi\left[-1+\left(1+\frac{8D}{k_\mathrm{B}A_w(k_n^\mathrm{o}, c_\mathrm{o})\xi^2}\right)^{1/2}\right], \qquad (11)$$

where function $A_w(k_n^\mathrm{o}, c_\mathrm{o})$ arises due to the consideration of energy of atoms „zero-point oscillations" in crystal:

$$A_w(k_n^\mathrm{o}, c_\mathrm{o}) = K_R\,\frac{5k_n^\mathrm{o}\,ab(b+1)}{144(b-a)}\left(\frac{r_\mathrm{o}}{c_\mathrm{o}}\right)^{b+2}, \qquad (12)$$

$$K_R = \frac{\hbar^2}{k_\mathrm{B}r_\mathrm{o}^2 m}, \quad \xi = \frac{9}{k_n^\mathrm{o}}.$$

Based on the potential (10), in the framework of the approximation of „only nearest neighbors interaction" for the equation of state (P) and the isothermal modulus of elasticity (B_T) one can obtain the following expressions [14]:

$$P = \left[\frac{k_n^\mathrm{o}}{6}D\,U'(R) + \frac{9}{4}k_\mathrm{B}\Theta_\mathrm{o}\gamma_\mathrm{o}E_w(y_w)\right]\frac{1}{v}, \qquad (13)$$

$$B_T = -v\left(\frac{\partial P}{\partial v}\right)_T = P + \left[\frac{k_n^\mathrm{o}}{18}D\,U''(R) + \frac{9}{4}k_\mathrm{B}\Theta_\mathrm{o} \times \gamma_\mathrm{o}(\gamma_\mathrm{o} - q_\mathrm{o})E_w(y_w) - 3k_\mathrm{B}\gamma_\mathrm{o}^2 T F_E(y_w)\right]\frac{1}{v}. \qquad (14)$$

Here $v = V/N$, $R = (v_0/v)^{1/3}$ — relative linear density of the crystal,

$$E_w(y_w) = 0.5 + \frac{1}{[\exp(y_w)-1]},$$

$$F_E(y_w) = \frac{y_w^2\exp(y_w)}{[\exp(y_w)-1]^2},$$

$$v_0 = \frac{\pi r_\mathrm{o}^2}{6k_p}, \quad U(R) = \frac{aR^b - bR^a}{b-a},$$

$$U'(R) = R\left[\frac{\partial U(R)}{\partial R}\right] = \frac{ab(R^b - R^a)}{b-a},$$

$$U''(R) = R\left[\frac{\partial U'(R)}{\partial R}\right] = \frac{ab(bR^b - aR^a)}{b-a}. \qquad (15)$$

From formula (11) it is easy to find expressions for the first (γ_o) and second (q_o) Grüneisen parameters for the vacancy-free crystal, which are

$$\gamma_\mathrm{o} = -\left(\frac{\partial \ln\Theta_\mathrm{o}}{\partial \ln v}\right)_T = \frac{b+2}{6(1+X_w)},$$

$$q_\mathrm{o} = \left(\frac{\partial \ln\gamma_\mathrm{o}}{\partial \ln v}\right)_T = \gamma_\mathrm{o}\frac{X_w(1+2X_w)}{(1+X_w)}. \qquad (16)$$

Here, the function $X_w = A_w\xi/\Theta_\mathrm{o}$ is introduced, which determines the role of quantum effects in calculating the Grüneisen parameters.

Since, according to (11), the Debye temperature does not depend on temperature during isochoric heating of the crystal, the isochoric heat capacity and isobaric coefficient of thermal volumetric expansion for the vacancy-free crystal can be determined in the form [15]:

$$C_v = 3Nk_\mathrm{B}F_E\left(\frac{3\Theta_\mathrm{o}}{4T}\right),$$

$$\alpha_p = \frac{1}{v}\left(\frac{\partial v}{\partial T}\right)_p = \gamma\frac{C_v}{VB_T} = \frac{\gamma C_v}{NB_T[\pi r_\mathrm{o}^3/(6k_p)]}\left(\frac{v_0}{v}\right). \qquad (17)$$

As was shown in [12], the method (1)–(17) allows, based on the parameters of the potential (10), to calculate both the temperature dependence along the isobar and the barometric dependence along the isotherm for all parameters of activation processes specified in formulas (7) and (8). This calculation method is applicable at any pressures and temperatures corresponding to the solid phase of a one-component substance.

2. Calculation results

Let us apply the formalism from (1)–(17) to calculate the activation parameters of iron ($m(\mathrm{Fe}) = 55.847$ amu) with different crystal structure. The change in the thermodynamic properties of iron at atmospheric pressure and temperature of α–γ-transition was studied by us in [16]. To study the properties of BCC-Fe and FCC-Fe in the article [16], the parameters of the Mie–Lennard-Jones (10) interatomic potential, which are presented in Table 1, were used. The right columns of the Table show the values of the molar volume, Debye temperature, thermal expansion coefficient, and modulus of elasticity calculated at $P = 0$ and $T = 300$ K. Experimental estimates of these parameters for BCC-Fe at $P = 0$ and $T = 300$ K are:

$$\Theta = 420 - 467\,\mathrm{K}\ [15],\ \alpha_p = (33-38)\cdot 10^{-6}\,\mathrm{K}^{-1}\ [17, 18],$$

$$B_T = 156 - 171\,\mathrm{GPa}\ [18, 19].$$

The comparison shows that our data are in good agreement with these estimates. A detailed study of the jumps in the iron properties during the α–γ-transition and comparison with the data of other authors were made by us [16].

Since the Curie temperature $T_\mathrm{C}(P = 0) = 1043$ K is only by 141 K lower than the temperature of the α–γ-transition $T_{\alpha-\gamma}(P = 0) = 1184 \pm 1$ K, this neighborhood makes it difficult to measure various thermodynamic properties at the α–γ-transition temperature, which was noted in papers [17,20,21]. The α–γ transition causes a very small change in volume and related properties:

$$\Delta v_{\alpha-\gamma} = v(\gamma) - v(\alpha) = -0.074\,\mathrm{cm}^3/\mathrm{mol}\ [22];$$

$$[v(\gamma) - v(\alpha)]/v(\alpha) = -0.0096 \approx -1\%\ [21].$$

Table 1. Parameters of Interatomic potential (10) for BCC and FCC iron structures from [16]

Phase	r_o, 10^{-10} m	D/k_B, K	b	a	v_0, cm^3/mol	$v(0,300\,\mathrm{K})$, cm^3/mol	$\Theta_o(0,300\,\mathrm{K})$, K	$\alpha_p(0,300\,\mathrm{K})$, $10^{-6}\mathrm{K}^{-1}$	$B_T(0,300\,\mathrm{K})$, GPa
α-bcc-Fe	2.4775	12561.530	8.37	3.09	7.0494	7.1339	415.174	34.117	161.291
γ-fcc-Fe	2.5404	8374.353	–	–	6.9812	7.0645	404.983	34.264	162.892

Note. After the parameters of the potential (10) other columns contain the calculated values of the molar volume, Debye temperature, thermal expansion coefficient and modulus of elasticity at $P = 0$ and $T = 300$ K.

Therefore, these jumps in properties during the $\alpha-\gamma$ transition are very difficult to measure. The matter is aggravated because of both the closeness of the Curie temperature and the fact that the measurement error of some properties is much greater than the magnitude of the jump in these properties during $\alpha-\gamma$ transition. For example, in [20, Fig. 5] it is shown that the change in the elasticity modulus (B_T) during the $\alpha-\gamma$-transition is less than the measurement error of B_T.

At the $\gamma-\delta$ transition temperature $T_{\gamma-\delta}(P=0) = 1667 \pm 1$ K, the volume change is also very small: $\Delta v_{\gamma-\delta} = v(\gamma)-v(\gamma) = 0.031\,\mathrm{cm}^3/\mathrm{mol}$ [22]. This is almost by an order of magnitude smaller than the jump in volume at the melting temperature of iron. Therefore, the change in various properties during the $\gamma-\delta$ phase transition is also very difficult to measure. In this connection, the experimental data available in the literature for activation parameters in various phases of iron are very approximate even for the self-diffusion enthalpy. Table 2 presents theoretical (in parentheses) and experimental estimates of activation parameters known from the literature in various phases of solid iron, which are given in the indicated articles. The first column also shows the temperature range in which the self-diffusion enthalpy h_d from the review [6] was measured. Thus, due to the difficulties in measuring activation parameters, the question of the activation parameters change during phase transitions in iron today does not have a clear answer even for such a relatively easily measurable activation parameter as the self-diffusion enthalpy.

Using the formalism (1)–(17) and the parameters of the interatomic potential (10) from Table 1, we calculated the activation parameters for BCC and FCC structures of iron. In this case, for α-Fe and δ-Fe the parameters of the potential (10) obtained for α-Fe were used. As was shown in [6,10], at the Curie temperature, the self-diffusion coefficient and the self-diffusion enthalpy change almost continuously within the accuracy of their measurement, i.e., without a jump. Therefore, the calculation of the α-Fe properties in the ferromagnetic and paramagnetic states was carried out on the basis of a single interatomic potential from Table 1.

Figs 1–4 show isobaric temperature dependences of the parameters both for the vacancy formation (two lower curves *1* and *2*), and for atom self-diffusion (two upper curves *3* and *4*) in the iron. The solid lines *1* and *3* show the $P = 0$ isobars, the dashed lines *2* and *4* — these are the $P = 10$ isobars, GPa. Vertical lines show the boundaries of various iron structures at $P = 0$. The values of activation parameters for BCC and FCC struc-

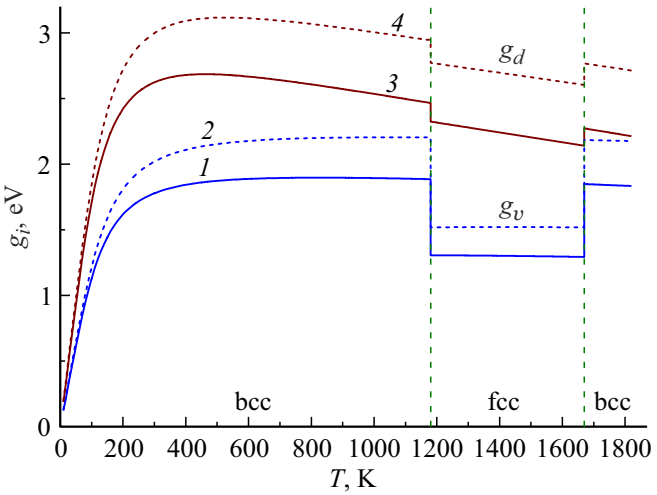

Figure 1. Isobaric temperature dependences of the Gibbs energy for vacancy formation (curves *1* and *2*) and for atom self-diffusion (curves *3* and *4*) in iron. Solid lines *1* and *3* — isobars $P = 0$, dashed lines *2* and *4* — isobars $P = 10$,GPa.

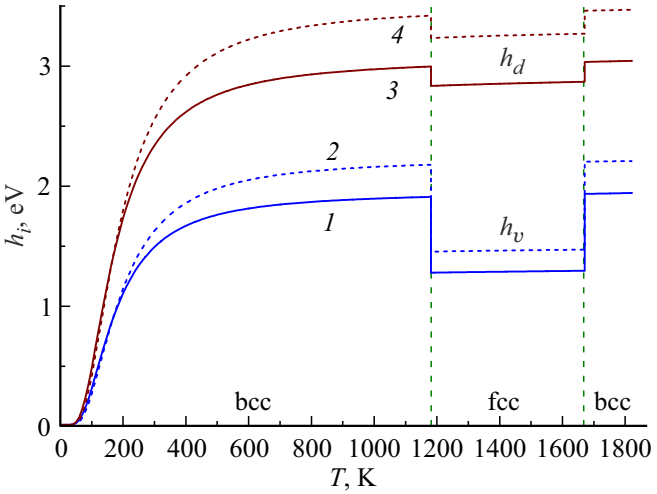

Figure 2. Temperature dependences of the enthalpy of vacancy formation (curves *1* and *2*) and self-diffusion (curves *3* and *4*) in iron. Lines *1* and *3* for $P = 0$, *2* and *4* — for $P = 10$ GPa.

Table 2. Theoretical (in parentheses) and experimental estimates of activation parameters in various phases of solid iron

Phase, measurement area	h_d, eV		h_v, eV		v_d/v_0		v_v/v_0	
α-bcc-Fe Ferromagnetic $T = 754-1043$ K	(2.788) 2.6−3.1	[6]	(1.30)	[3]			(0.50) 0.95	[3]
	(2.92) 2.63−3.10	[10]	(2.20)	[10]				
	2.634	[24]	1.81 ± 0.1	[25]				
α-bcc-Fe Paramagnet $T = 1052-1148$ K	(2..05−2.47) 2.35−3.0	[4]	(1.37−1.70) 1.6−1.8	[4]	(6.27−0.899)	[4]	(0.703−0.939) 0.95	[4]
	(2.446) 2.48−2.68	[6]	(2.16−2.64)	[7]			(0.63)	[3]
	(3.052) 2.36−3.01	[9]	(2.370) 1.59−2.0	[9]	(0.723)	[9]	(0.744) 0.95	[9]
	(2.46) 2.48−2.92	[10]	(1.99)	[10]				
	2.5−2.7	[24]	(1.98) 1.6 ± 0.2	[23]				
	2.88	[25]	1.74 ± 0.1	[25]				
γ-fcc-Fe $T = 1443-1634$ K	(3.93) 2.94	[6]	(2.65)	[3]			(0.70)	[3]
	2.942 ± 0.063	[24,26]					(0.74) 0.77	[26]
δ-bcc-Fe $T = 1443-1634$ K	(2.083) 2.33−2.53	[6]						
	2.5−2.7	[24]						

Note. The first column shows the temperature range in which the self-diffusion enthalpy was measured from [6].

tures of iron at certain temperatures are presented in Table 3−6: 300, $T_{\alpha-\gamma}(P=0) = 1184$, $T_{\gamma-\delta}(P=0) = 1667$, $T_m(P=0) = 1810$ K. For each phase the first line presents the data obtained at $P = 0$, and the second line — at $P = 10$ GPa. Note that in Fig. 4 and Tables 3−6 for the normalization volume v_0 in different Fe structures different values from Table 1 were used.

It can be seen from Figs. 2 and 4 and Tables 3−6 that our results for h_i and v_i/v_0 at high temperatures ($T \gg \Theta_{texto}$) are in good agreement with the experimental estimates of these functions presented in Table 2. We were unable to find experimental or theoretical estimates of the functions s_i and $g_i = h_i - Ts_i$ for various phases of iron in the literature.

It can be seen from Fig. 1−4 that at low temperatures, due to quantum laws, the activation parameters strongly depend on temperature, and the entropy of the activation process in this region is negative: $s_i(T < \Theta_o) < 0$. At $T = 0$ K the parameters of the activation process reach their minima:

$$g_i(0) = 0, \quad h_i(0) = 0, \quad v_i(0) = 0, \quad s_i(0) < 0.$$

The reasons for this behavior of these functions were discussed in detail in [12]. Note that the negative entropy of the activation process was found at low temperatures both in experimental [27,28] and theoretical [29–31] studies.

It can be seen from Figs 1−4 and Table 4 that at the $\alpha-\gamma$-transition temperature (1184 K) the activation parameters decrease during the isobaric transition from BCC to FCC structure. In this case, if the self-diffusion parameters decrease by 4−6%, then the vacancy parameters decrease by 31−34%. As the pressure increases, the jump of the g_i and h_i functions increases, and the jump of s_i and v_i — functions decreases. Note that the increase in h_v and the decrease in v_v with increasing pressure were studied experimentally for FCC Au, Al, Pt in [32] and theoretically for BCC-Ta in [33].

Note that the accuracy of the experimental determination of these functions does not allow today to measure such jumps in activation parameters. As for theoretical calculations, then in article [6] the self-diffusion coefficients in various polymorphic phases of iron were calculated on the basis of the thermodynamic cBΩ model, and increase in the self-diffusion enthalpy during $\alpha-\gamma$-transition from 2.446 to 3.93 eV (Table 2) was obtained. However, this is much higher than the experimental value: $h_d(\gamma\text{-Fe}) = 2.94$ eV. In

Table 3. Activation parameters for BCC and FCC iron structures calculated at $T = 300$ K and two pressures — 0 and 10 GPa

Phase	P, GPa	$-\lg(x_d)$	$-\lg(\phi_v)$	g_d, eV	g_v, eV	h_d, eV	h_v, eV	s_d/k_B	s_v/k_B	v_d/v_0	v_v/v_0	v_d, cm^3/mol	v_v, cm^3/mol
α-bcc-Fe	0	44.09	29.87	2.623	1.778	2.327	1.480	−11.443	−11.508	0.5699	0.3625	4.0173	2.5555
	10	50.38	33.93	2.999	2.020	2.550	1.622	−7.352	−15.373	0.4718	0.3001	3.3257	2.1156
γ-fcc-Fe	0	41.78	20.30	2.487	1.208	2.227	0.999	−10.059	−8.077	0.5434	0.2439	3.7934	1.7024
	10	47.74	23.01	2.842	1.370	2.443	1.096	−15.410	−10.572	0.4513	0.2025	3.15029	1.4138

Table 4. Activation parameters for BCC-Fe and FCC-Fe calculated at $T_{\alpha-\gamma}(P = 0) = 1184$ K and two pressures — 0 and 10 GPa

Phase	P, GPa	$-\lg(x_d)$	$-\lg(\phi_v)$	g_d, eV	g_v, eV	h_d, eV	h_v, eV	s_d/k_B	s_v/k_B	v_d/v_0	v_v/v_0	v_d, cm^3/mol	v_v, cm^3/mol
α-bcc-Fe	0	10.49	8.02	2.464	1.885	2.983	1.898	5.089	0.124	0.7347	0.4674	5.1794	3.2947
	10	12.52	9.38	2.942	2.203	3.414	2.172	4.628	−0.303	0.6106	0.3884	4.3043	2.7381
γ-fcc-Fe	0	9.89	5.56	2.323	1.306	2.822	1.266	4.893	−0.387	0.6949	0.3119	4.8515	2.1773
	10	11.79	6.46	2.770	1.519	3.226	1.448	4.471	−0.693	0.5784	0.2596	4.0380	1.8122

Table 5. Activation parameters for FCC-Fe and BCC-Fe calculated at $T_{\gamma-\delta}(P = 0) = 1667$ K and two values of pressure — 0 and 10 GPa

Phase	P, GPa	$-\lg(x_d)$	$-\lg(\phi_v)$	g_d, eV	g_v, eV	h_d, eV	h_v, eV	s_d/k_B	s_v/k_B	v_d/v_0	v_v/v_0	v_d, cm^3/mol	v_v, cm^3/mol
γ-fcc-Fe	0	6.47	3.91	2.141	1.293	2.856	1.283	4.978	−0.071	0.7337	0.3295	5.1219	2.3003
	10	7.87	4.59	2.604	1.519	3.262	1.464	4.581	−0.380	0.5994	0.2690	4.1845	1.8780
δ-bcc-Fe	0	6.87	5.59	2.274	1.848	3.021	1.922	5.201	0.514	0.7759	0.4937	5.4699	3.4806
	10	8.37	6.60	2.769	2.184	3.454	2.197	4.770	0.090	0.6329	0.4026	4.4615	2.8381

Table 6. Activation parameters for FCC-Fe and BCC-Fe calculated at $T = 1810$ K and two values of pressure — 0 and 10 GPa

Phase	P, GPa	$-\lg(x_d)$	$-\lg(\phi_v)$	g_d, eV	g_v, eV	h_d, eV	h_v, eV	s_d/k_B	s_v/k_B	v_d/v_0	v_v/v_0	v_d, cm^3/mol	v_v, cm^3/mol
γ-fcc-Fe	0	5.80	3.58	2.082	1.287	2.865	1.289	5.014	0.015	0.7458	0.3356	5.2066	2.3428
	10	7.12	4.22	2.555	1.517	3.269	1.467	4.577	−0.315	0.6053	0.2717	4.2258	1.8969
δ-bcc-Fe	0	6.17	5.11	2.217	1.835	3.030	1.930	5.209	0.610	0.7888	0.5024	5.5606	3.5417
	10	7.57	6.06	2.717	2.176	3.461	2.202	4.771	0.166	0.6392	0.4066	4.5058	2.8665

the article [6] by the same cBΩ method the reduce in the self-diffusion volume from $(5.22-5.26)$ cm^3/mol for α-Fe to $(4.17-4.97)$ cm^3/mol for γ-Fe. was obtained. This result agrees well with our calculations from Table 4.

It can be seen from Figs. 1–4 and Table 5 that at the $\gamma-\delta$-transition temperature (1667 K) the activation parameters increase during the isobaric transition from the FCC to BCC structure. The self-diffusion parameters increase by 4–6%, and the vacancy parameters increase by 40–70%. As the pressure increases, the jump of the g_i and h_i functions increases, while the jump of the s_i and v_i functions decreases. And during $\gamma-\delta$-transition, the accuracy of the experimental determination of these functions is not very high. There are two experimental studies relating measuring the self-diffusion coefficient in δ-Fe. In [34] in the region $T = 1663-1783$ K the following was obtained: $h_d = 57 \pm 3$ kcal/mol $= 2.473 \pm 0.13$ eV. In [35] for self-diffusion in the paramagnetic α-Fe phase (for $T = 956-1157$ K) and in δ-Fe (for $T = 1701-1765$ K), the same self-diffusion enthalpy $h_d = 57.5 \pm 1.04$ kcal/mol $= 2.495 \pm 0.045$ eV was obtained. In this case, the self-diffusion coefficient itself in [35] was measured with an accuracy of 22%. As for theoretical calculations, in the article [6], on the basis of the thermodynamic cBΩ model, the decrease in the self-diffusion enthalpy during $\gamma-\delta$ transition in iron from 3.93 to 2.083 eV (Table 2) was obtained. However, these calculated values differ significantly from

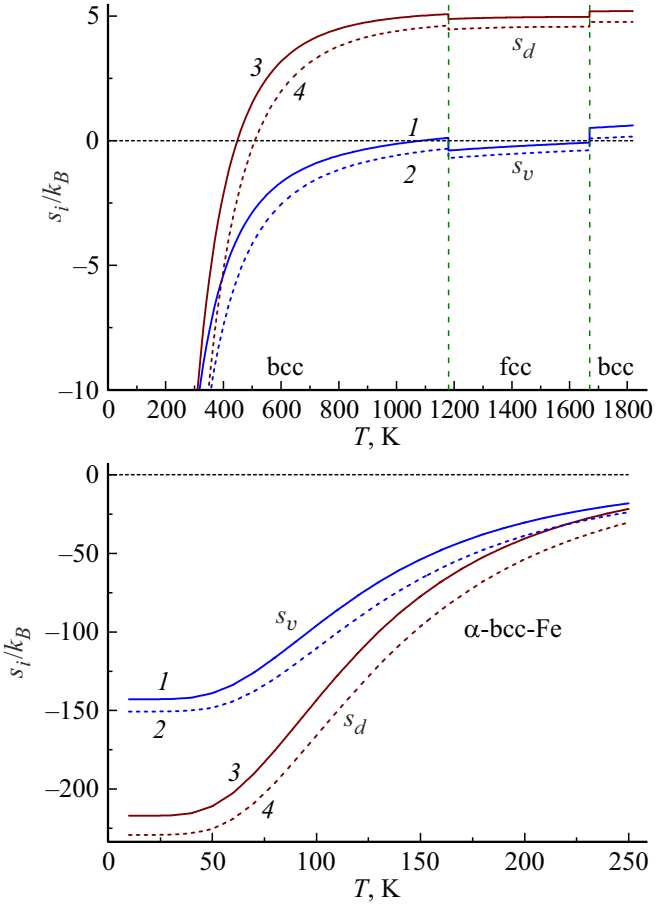

Figure 3. Temperature dependences of the entropy of vacancy formation (curves *1*and *2*) and self-diffusion (curves *3* and *4*) in iron. Solid lines *1* and *3* — isobars $P = 0$, dashed lines *2* and *4* — isobars $P = 10$ GPa. The bottom graph shows these dependences in ow temperature range for BCC-Fe.

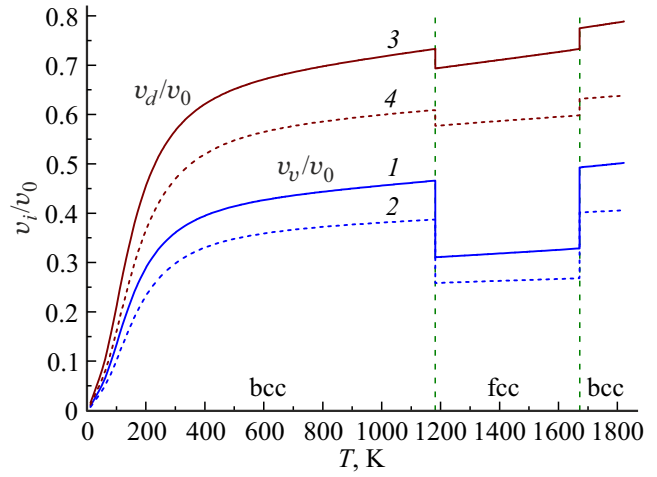

Figure 4. Temperature dependences of the normalized volume of vacancy formation (lines *1* and *2*) and self-diffusion (lines *3* and *4*). Lines *1* and *3* for $P = 0$, *2* and *4* — for $P = 10$ GPa.

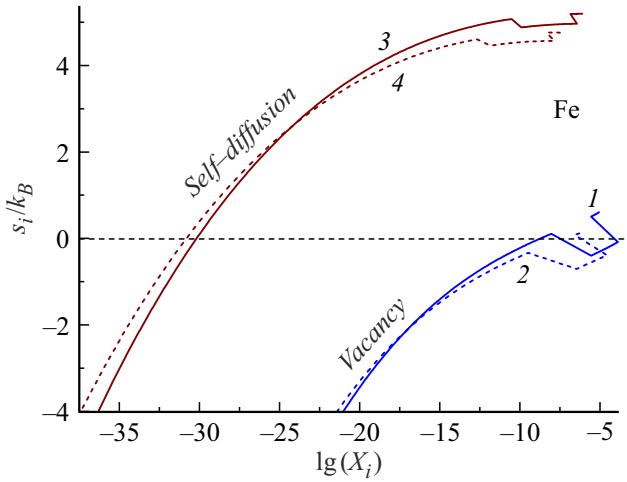

Figure 5. Isobar dependences of the entropy of vacancy formation (curves *1* and *2*) and self-diffusion (curves *3* and *4*) on the logarithm of the vacancy concentration and delocalized atoms in iron. Lines *1* and *3* for $P = 0$, *2* and *4* — for $P = 10$ GPa.

the experimental estimates for h_d. The self-diffusion volume increasing from $(4.17-4.97)\,\mathrm{cm}^3/\mathrm{mol}$ for γ-Fe up to $(4.99-5.08)\,\mathrm{cm}^3/\mathrm{mol}$ for δ-Fe was also obtained. This result agrees well with our calculations from Table 5. We failed to find experimental or theoretical data on vacancy parameters for δ-Fe.

Fig. 5 shows the dependences of the entropy of the vacancy formation (curves *1* and *2*) and self-diffusion (curves *3* and *4*) on the decimal logarithm concentration of vacancies and delocalized atoms in iron. It can be seen from Fig. 5 that as the concentration of defects decreases, the entropy corresponding to them becomes negative, i.e. in this region these defects order the crystal. Only starting from a certain concentration (X_{si}) the entropy of defect formation transfers to positive region, where the defects disorder the crystal. The reasons for this behavior of s_i function were discussed in detail in [36,37]. It can be seen from Fig. 5 that diffusing atoms begin to disorder the crystal at lower concentrations than vacancies. Thus, the following relation is satisfied: $X_{sd} < X_{sv}$, and with pressure increasing the value X_{sd} decreases, while the value X_{sv} increases.

As can be seen from Figs 3 and 5, during the $\alpha-\gamma$-transition the entropy of defects decreases sharply, and the entropy of vacancy formation in γ-Fe is negative, i.e. here, vacancies order the crystal. During the $\gamma-\delta$ transition the entropy of defect formation increases, and in δ-Fe the vacancies, like delocalized atoms, disorder the crystal.

As can be seen from Fig. 5, the entropy of defect formation in iron becomes negative at a very low concentration of defects: $X_{si} < 10^{-8}$ (for vacancies) — 10^{-30} (for diffusing atoms). But for such crystals as, for example, ^{3}He, ^{4}He, H_2, D_2, Ne, Li, the change of sign of the vacancy formation entropy occurs at a more noticeable concentration of defects [36]. That is why the negative value of the

vacancy formation entropy was experimentally found in helium crystals in [27,28].

Conclusion

1. Analytical method based on the pair four-parameter potential of interatomic interaction of Mie−Lennard-Jones calculated the isobaric temperature dependence of activation parameters for BCC and FCC iron structures from $T = 10$ to 1810 K along two isobars — $P = 0$ and 10 GPa.

2. For the first time, according to a single method all parameters of activation processes were calculated: the Gibbs energy, enthalpy, entropy, and volume both for the process of vacancy formation and for the process of self-diffusion. It is shown that the temperature dependence of activation parameters at low temperatures ($T < \Theta$) is quite considerable due to quantum effects. The temperature dependence of activation parameters at high temperatures weakens and is almost linear. In the region of high temperatures good agreement is obtained with experimental estimates of activation parameters known from the literature for various iron structures.

3. It is shown that at the $\alpha-\gamma$-transition temperature, the activation parameters decrease during the isobaric transition from the BCC to FCC structure. At the $\gamma-\delta$-transition temperature, the activation parameters increase during the isobaric transition from the FCC to the BCC structure. With pressure increasing the magnitude of the jumps for the Gibbs energy and the enthalpy of the activation process increases, while decreases for the entropy and volume of the activation process.

4. At low concentration of defects (i.e., at low temperatures), the entropy of defect formation becomes negative, i.e., they order the crystal here. Only starting from a certain concentration (X_{si}) the entropy of defect formation transfers to positive region, where the defects disorder the crystal. In this case, diffusing atoms begin to disorder the crystal at lower concentrations than vacancies, i.e., $X_{sd} < X_{sv}$, and with pressure increasing the value of X_{sd} decreases, and the value of X_{sv} increases.

Acknowledgments

The author wishes to thank S.P. Kramynin, N.Sh. Gazanova, Z.M. Surkhaeva, and M.M. Gadzhieva for fruitful discussions and their help.

Conflict of interest

The author declares that he has no conflict of interest.

References

[1] P.I. Dorogokupets, A.M. Dymshits, K.D. Litasov, T.S. Sokolova. Scientific Reports, **7** (1), 1 (2017). DOI: 10.1038/srep41863
[2] S.J. Turneaure, S.M. Sharma, Y.M. Gupta. Phys. Rev. Lett., **125** (21), 215702 (2020). DOI: 10.1103/PhysRevLett.125.215702
[3] P.A. Korzhavyi, I.A. Abrikosov, B. Johansson, A.V. Ruban, H.L. Skriver. Phys. Rev. B, **59** (18), 11693 (1999). DOI: 10.1103/PhysRevB.59.11693
[4] I.V. Valikova, A.V. Nazarov. Phys. Metals Metallography, **109** (3), 220 (2010). DOI: 10.1134/S0031918X10030026
[5] R. Nazarov, T. Hickel, J. Neugebauer. Phys. Rev. B, **85** (14), 144118 (2012). DOI: 10.1103/PhysRevB.85.144118
[6] B.H. Zhang. AIP Advances, **4** (1), 017128 (2014). DOI: 10.1063/1.4863462
[7] B. Medasani, M. Haranczyk, A. Canning, M. Asta. Comp. Mater. Sci., **101**, 96 (2015). DOI: 10.1016/j.commatsci.2015.01.018
[8] Y. Gong, B. Grabowski, A. Glensk, F. Körmann, J. Neugebauer, R.C. Reed. Phys. Rev. B, **97** (21), 214106 (2018). DOI: 10.1103/PhysRevB.97.214106
[9] P.-W. Ma, S.L. Dudarev. Phys. Rev. Mater., **3** (6), 063601 (2019). DOI: 10.1103/physrevmaterials.3.063601
[10] A. Schneider, C.C. Fu, F. Soisson, C. Barreteau. Phys. Rev. Lett., **124** (21), 215901 (2020). DOI: 10.1103/PhysRevLett.124.215901
[11] P.A. Varotsos, N.V. Sarlis, E.S. Skordas. Crystals, **12** (5), 686 (2022). DOI: 10.3390/cryst12050686
[12] M.N. Magomedov. Physica Solid State, **64** (4), 469 (2022). DOI: 10.21883/PSS.2022.04.53504.240
[13] M.N. Magomedov. Tech. Phys., **58** (9), 1297 (2013). DOI: 10.1134/S106378421309020X
[14] M.N. Magomedov. Physics Solid State, **64** (7), 765 (2022). DOI: 10.21883/PSS.2022.07.54579.319
[15] L.A. Girifalco. *Statistical Physics of Materials* (J. Wiley and Sons Ltd., NY., 1973)
[16] M.N. Magomedov. Physics Solid State, **63** (2), 215 (2021). DOI: 10.1134/S1063783421020165
[17] S.I. Novikova. *Teplovoe rasshirenie tverdykh tel* (Nauka, M., 1974) (in Russian).
[18] D.R. Wilburn, W.A. Bassett. American Mineralogist, **63** (5–6), 591 (1978). https://pubs.geoscienceworld.org/msa/ammin/article-abstract/63/5-6/591/40926
[19] Y. Shibazaki, K. Nishida, Y. Higo, M. Igarashi, M. Tahara, T. Sakamaki, H. Terasaki, Y. Shimoyama, S. Kuwabara, Y. Takubo, E. Ohtani. American Mineralogist, **101** (5), 1150 (2016). DOI: 10.2138/am-2016-5545
[20] Z. Dong, W. Li, D. Chen, S. Schönecker, M. Long, L. Vitos. Phys. Rev. B, **95** (5), 054426 (2017). DOI: 10.1103/PhysRevB.95.054426
[21] A.M. Balagurov, I.A. Bobrikov, I.S. Golovin. JETP Lett., **107** (9), 558 (2018). DOI: 10.7868/S0370274X18090084
[22] L.J. Swartzendruber. Bulletin of Alloy Phase Diagrams, **3** (2), 161 (1982). DOI: 10.1007/BF02892374
[23] U. Krause, J.P. Kuska, R. Wedell. Phys. Stat. Sol. (b), **151** (2), 479 (1989). DOI: 10.1002/pssb.2221510208
[24] *Metals Reference Book,* C.I. Smithells (Butterworth and Co. (Publishers) Ltd., London, 1976)
[25] H.E. Schaefer. Phys. Stat. Sol. (a), **102** (1), 47 (1987). DOI: 10.1002/pssa.2211020104
[26] T. Heumann, R. Imm. J. Phys. Chem. Sol., **29** (9), 1613 (1968). DOI: 10.1016/0022-3697(68)90103-0
[27] P.R. Granfors, B.A. Fraass, R.O. Simmons. J. Low Temperature Phys., **67** (5/6), 353 (1987). DOI: 10.1007/BF00710349

[28] I. Iwasa. J. Phys. Society Jpn., **56** (5), 1635 (1987). DOI: 10.1143/JPSJ.56.1635
[29] M.I. Mendelev, B.S. Bokstein. Philosophical Magazine, **90** (5), 637 (2010). DOI: 10.1080/14786430903219020
[30] C.Z. Hargather, S.-L. Shang, Z.-K. Liu, Y. Du. Computational Mater. Sci., **86**, 17 (2014). DOI: 10.1016/j.commatsci.2014.01.003
[31] N.P. Kobelev, V.A. Khonik. JETP, **126** (3), 340 (2018). DOI: 10.1134/S1063776118030032
[32] M. Senoo, H. Mii, I. Fujishiro, T. Takeuchi. Jpn. J. Appl. Phys., **12** (10), 1621 (1973). DOI: 10.1143/JJAP.12.1621
[33] S. Mukherjee, R.E. Cohen, O. Gülseren. J. Phys.: Condens. Matter., **15** (6), 855 (2003). DOI: 10.1088/0953-8984/15/6/312
[34] R.J. Borg, D.Y.F. Lai, O.H. Krikorian. Acta Metallurgica, **11** (8), 867 (1963). DOI: 10.1016/0001-6160(63)90056-7
[35] D.W. James, G.M. Leak. A J. Theor. Experiment. Appl. Phys., **14** (130), 701 (1966). DOI: 10.1080/14786436608211966
[36] M.N. Magomedov. Tech. Phys. Lett., **28** (5), 430 (2002). DOI: 10.1134/1.1482758
[37] M.N. Magomedov. Tech. Phys. Lett., **48** (6), 59 (2022). DOI: 10.21883/TPL.2022.06.53793.19234